

Solvent Effects on the Excited-State Processes of Protochlorophyllide: A Femtosecond Time-Resolved Absorption Study

B. Dietzek,[†] W. Kiefer,[†] G. Hermann,[‡] J. Popp,[§] and M. Schmitt^{*,§}

Institut für Physikalische Chemie, Bayerische Julius-Maximilians Universität Würzburg, Am Hubland, 97074 Würzburg, Germany, Institut für Biophysik und Biochemie, Friedrich-Schiller-Universität Jena, Philosophenweg 12, 07743 Jena, Germany, and Institut für Physikalische Chemie, Friedrich-Schiller-Universität Jena, Helmholtzweg 4, 07743 Jena, Germany

Received: October 4, 2005; In Final Form: December 12, 2005

The excited-state dynamics of protochlorophyllide a, a porphyrin-like compound and, as substrate of the NADPH/protochlorophyllide oxidoreductase, a precursor of chlorophyll biosynthesis, is studied by femtosecond absorption spectroscopy in a variety of solvents, which were chosen to mimic different environmental conditions in the oxidoreductase complex. In the polar solvents methanol and acetonitrile, the excited-state dynamics differs significantly from that in the nonpolar solvent cyclohexane. In methanol and acetonitrile, the relaxation dynamics is multiexponential with three distinguishable time scales of 4.0–4.5 ps for vibrational relaxation and vibrational energy redistribution of the initially excited S_1 state, 22–27 ps for the formation of an intermediate state, most likely with a charge transfer character, and 200 ps for the decay of this intermediate state back to the ground state. In the nonpolar solvent cyclohexane, only the 4.5 ps relaxational process can be observed, whereas the intermediate intramolecular charge transfer state is not populated any longer. In addition to polarity, solvent viscosity also affects the excited-state processes. Upon increasing the viscosity by adding up to 60% glycerol to a methanolic solution, a deceleration of the 4 and 22 ps decay rates from the values in pure methanol is found. Apparently not only vibrational cooling of the S_1 excited state is slowed in the more viscous surrounding, but the formation rate of the intramolecular charge transfer state is also reduced, suggesting that nuclear motions along a reaction coordinate are involved in the charge transfer. The results of the present study further specify the model of the excited-state dynamics in protochlorophyllide a as recently suggested (*Chem. Phys. Lett.* **2004**, 397, 110).

Introduction

Protochlorophyllide a (Pchlde a) belongs to the class of porphyrin compounds which are of significant biological importance. Pchlde a is a Mg-tetrapyrrole made up of four pyrrole-type rings, linked together by four methine bridges (Figure 1). It is one of the key intermediates in the biosynthesis of chlorophyll and is synthesized from δ aminolevulinic acid by enzyme catalysis.^{1–3} In a subsequent reaction step, Pchlde a is reduced at the C-17, C-18 double bond of ring D to yield the chlorine macrocycle of chlorophyllide a, from which chlorophyll a is finally derived by esterification of the C-17 propionyl group with the polyisoprene alcohol phytol. The reduction of Pchlde a is catalyzed by two distinct enzymes, the light-dependent and light-independent NADPH/protochlorophyllide oxidoreductase (POR).^{4–6} Both of these enzymes are widely distributed among phototrophic organisms. While in most of the oxygenic photosynthetic organisms the two enzymes coexist with each other, angiosperms appear to use only the light-dependent pathway and anoxygenic photosynthetic bacteria only the light-independent pathway. The light-dependent POR enzyme not only is of importance as a key regulator of chlorophyll synthesis but also is one of only two enzymes in which catalytic activity is initiated by the absorption of light. The requirement for light makes the POR enzyme an attractive

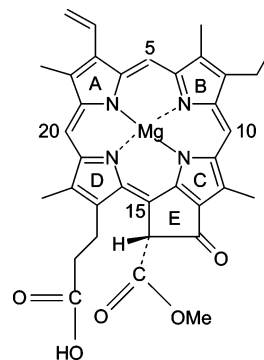


Figure 1. Chemical structure of protochlorophyllide a.

model for studying the molecular events of an enzymatic reaction in real time by use of time-resolved spectroscopy. Thus, the first femtosecond study on the ultrafast reaction dynamics in the POR enzyme, a ternary complex between the apoprotein, the substrate Pchlde a, and the coenzyme NADPH, was reported recently.⁷

We have initiated a study on the excited-state chemistry of the substrate Pchlde a in solution separated from the apoprotein. By assessing the internal excited-state dynamics of the isolated substrate, we hope to facilitate understanding of the more complex processes in the ternary enzyme complex and to unravel the role of the apoprotein in driving the enzymatic reaction toward the product with high selectivity and efficiency. In a preceding letter,⁸ we have already shown that the excited-state decay of Pchlde a occurs via two decay channels, one leading to an immediate repopulation of the ground state and the other

* Corresponding author. Phone: (+49-3641) 948 367. Fax: (+49-3641) 948 302. E-mail: m.schmitt@uni-jena.de.

[†] Bayerische Julius-Maximilians Universität Würzburg.

[‡] Institut für Biophysik und Biochemie, Friedrich-Schiller-Universität Jena.

[§] Institut für Physikalische Chemie, Friedrich-Schiller-Universität Jena.

creating an intermediate state with a time constant of 27 ps, which in turn decays into the ground state with a 200 ps time constant. Here, we study the effects of different solvents, varying in polarity, viscosity, and protic properties, on the routing of the excitation energy into the two different deactivation channels. Under the assumption that the solvent conditions can mimic specific environmental conditions, interactions may possibly be identified, which control the catalysis in the native enzyme complex. The results show that the excited-state processes of Pchl *a* are strongly affected by the solvent polarity, indicating that this solvent property is an important factor in determining the dynamic behavior of the S_1 excited state. Further, while the protic properties of the solvent have no effect on the excited-state relaxations, an increase in the solvent viscosity slows down an ultrafast 4 ps vibrational relaxation/cooling process in the S_1 state and, in addition, the 27 ps kinetics populating the intermediate state. It thus appears that not only is vibrational cooling slowed by the higher viscous medium, but the formation of the intermediate state is as well, possibly due to viscosity-dependent nuclear rearrangements along a reaction coordinate. Taken all together, the data presented here verify the kinetic model suggested recently for the excited-state dynamics of Pchl *a*⁸ and offer a more complete description of the initial kinetic processes.

Experimental Section

Instrumentation and Measuring Procedure. The laser system used to perform the time-resolved transient absorption (TA) measurements has been described in detail elsewhere.⁹ In brief, a titanium:sapphire oscillator (MIRA, Coherent) and an amplifier system (MXR/CPA 1000, Clark) generated femtosecond laser pulses with a full width at half-maximum (fwhm) of 80 fs and an energy of approximately 1.0 mJ per pulse at a repetition rate of 1 kHz. This amplified 800 nm output was split into two parts by means of a 1:1 beam splitter. One part was used to pump a four pass optical parametric amplifier (TOPAS, Light Conversion) to generate the tunable pump pulses. The OPA pulses were chirp compensated and compressed to 90 fs. The second part of the amplified 800 nm output was used to generate a white light continuum in a 3 mm sapphire window. The polarization of the pump beam and the white light continuum were chosen to be at the magic angle. The chirp of the white light continuum was numerically compensated to <0.2 fs/nm in the course of data processing. Thus, the time resolution obtained in the spectral region of our experiments was about 100 fs. The changes in the absorption of the sample were measured as the difference of the optical density between the sample with and without excitation. To avoid thermal effects, the sample was rotated in a rotating cell and the rotation speed was adjusted so that each laser pulse excited a fresh sample volume. A typical data run consisted of 10 scans during each 200 pulses were accumulated at each delay time to compensate for the statistical fluctuations of the probe and pump light. Further, at least three different series of experiments were carried out. Room temperature measurements were carried out with samples, which were freshly diluted in the desired solvent to give an optical density of ~ 0.3 at the absorption maximum in a 1 mm optical path length (corresponding to a concentration of $\sim 1 \times 10^{-4}$ mol/L with the exact value depending on the solvent). Stationary absorption spectra were recorded before and after each measurement to check the integrity of the sample. The steady-state absorption spectra were taken with a Lambda19 spectrometer (Perkin-Elmer). The steady-state fluorescence spectra were monitored with a Fluorolog III spectrofluorometer (Jobin Yvon).

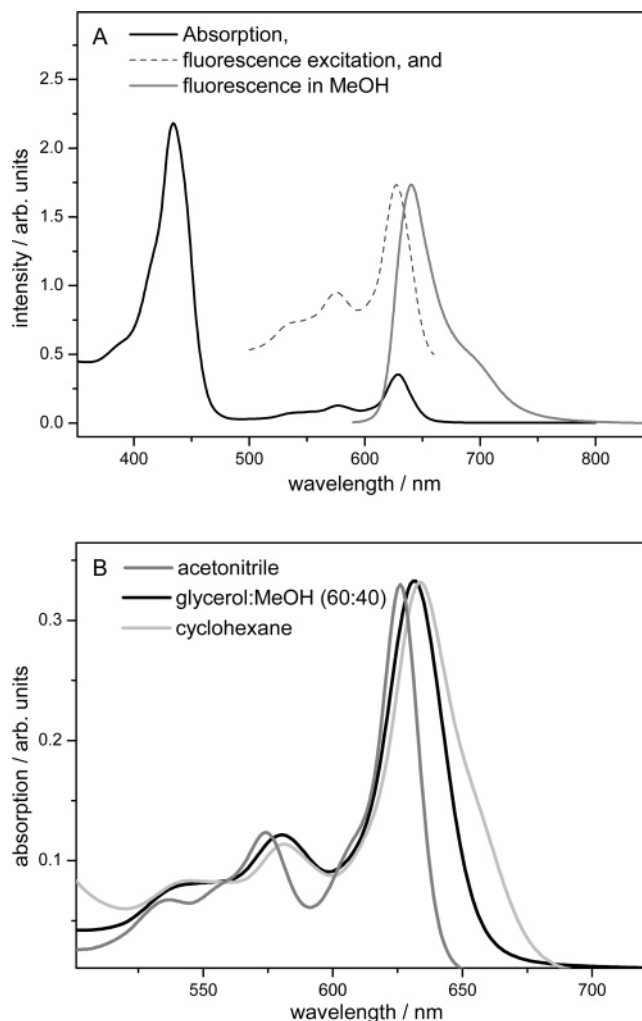


Figure 2. Steady-state absorption, fluorescence, and fluorescence excitation spectra of protochlorophyllide *a*: (A) steady-state absorption, fluorescence ($\lambda_{\text{exc}} = 627$ nm), and fluorescence excitation ($\lambda_{\text{em}} = 641$ nm) spectra of protochlorophyllide *a* in methanol at room temperature; (B) steady-state absorption spectra in different solvents. The visible absorption within the region of the Q bands is shown for the solvents acetonitrile, methanol/glycerol (40/60), and cyclohexane. The spectra are normalized to the same relative maximum absorbance.

Preparation of Protochlorophyllide *a*. Pchl *a* was purified from etiolated oat seedlings (*Avena sativa* L. cv Tomba) fed with 35 mM 5-aminolevulinic acid according to a method reported by Klement et al.¹⁰ Freshly prepared samples were dried in a slow stream of argon and stored in evacuated glass vessels at 250 K. The purity of the isolated Pchl *a* was detected by analytical HPLC using a Hewlett-Agilent 1100 apparatus equipped with a LCQ mass spectrometer (Finnigan). Pchl *a* was eluted from a RP-18 column (125 mm \times 2 mm, 3 μ m particle size) with a gradient of acetonitrile starting from 50% acetonitrile in 0.1% TFA and increasing to 100% acetonitrile in 0.1% TFA within 15 min. Detection was carried out at 420 nm. Pchl *a* was eluted with a m/z peak of 591.7 g/mol. This m/z peak corresponds with the molecular mass expected for Pchl *a* when it is taken into account that the Mg^{2+} has been lost under the separation conditions.

Results and Discussion

Steady-State Absorption Spectra. Figure 2 depicts the steady-state absorption spectrum of Pchl *a* in different solvents including the fluorescence and fluorescence excitation

TABLE 1: Time Constants of the Kinetic Processes in Excited-State Pchlde a Measured in Various Solvents^a

solvent	$P(\epsilon)$	η/cp	τ_1/ps	τ_2/ps	τ_3/ps
methanol	0.913	0.597	4.0 ± 1.0	27 ± 6	200 ± 60
acetonitrile	0.921	0.345	4.5 ± 1.2	22 ± 4	200 ± 60
cyclohexane	0.254	0.660	4.5 ± 1.8		
methanol/glycerol (40/60)	0.927	44.902	12.1 ± 2.6	40 ± 7	270 ± 70

^a The time constants were obtained from a triexponential fit except for the solvent cyclohexane, which was best fitted by a monoexponential function. The solvent polarity, P , was determined from the dielectric constant, ϵ , according to the expression $P(\epsilon) = (\epsilon - 1)/(\epsilon + 2)$. All of the listed parameters represent values at 293.15 K.

spectra in methanol. The absorption spectra share the same spectral features as those of porphyrins¹¹ with a strong Soret band at 434 nm and three weaker Q absorption bands at 534, 576, and 629 nm in the solvent methanol. The fluorescence spectrum exhibits a comparatively small red shift relative to the absorption spectrum with a maximum at 640 nm and with excitation maxima matching the absorption peaks. The close resemblance between the absorption and fluorescence excitation spectra indicates the high purity of the Pchlde a samples studied in the time-resolved measurements. Further, the spectral features revealed in methanol agree well with those reported recently.¹² Figure 2B compares the spectra of Pchlde a in solvents, which

differ in their polarity, protic properties, and viscosity. As compared to the spectrum in methanol, in the highly polar but aprotic solvent acetonitrile, the Q bands appear slightly blue-shifted with a decrease in the width (fwhm) of the main absorption at 626 nm from 28 nm in methanol to 20 nm in acetonitrile and an increasingly resolved vibronic structure. In contrast, in the nonpolar and aprotic solvent cyclohexane, the Q bands shift to the red relative to those in methanol, with a peak at 634 nm, while the width in this main absorption band increases to 34 nm. An increase in the solvent viscosity by adding up to 60% glycerol to the methanolic solution and thus maintaining the gross solvent polarity (see Table 1) does not affect the absorption spectrum significantly. Similar to the spectrum in methanol, the Q bands exhibit peaks at 538, 580, and 631 nm and are closely related in their pattern to the well-resolved Q band structure in pure methanol. This clearly demonstrates that the electronic structure of Pchlde a is retained in the methanol/glycerol mixture and that the addition of glycerol only affects the solvent viscosity.

Effects of Different Solvents on the Excited-State Dynamics. On the basis of the differing steady-state absorption spectra of Pchlde a depending on the particular solvent environment, a distinct influence of the solvent properties on the excited-state dynamics can be expected. For further insight into these dynamics, time-resolved absorption measurements were per-

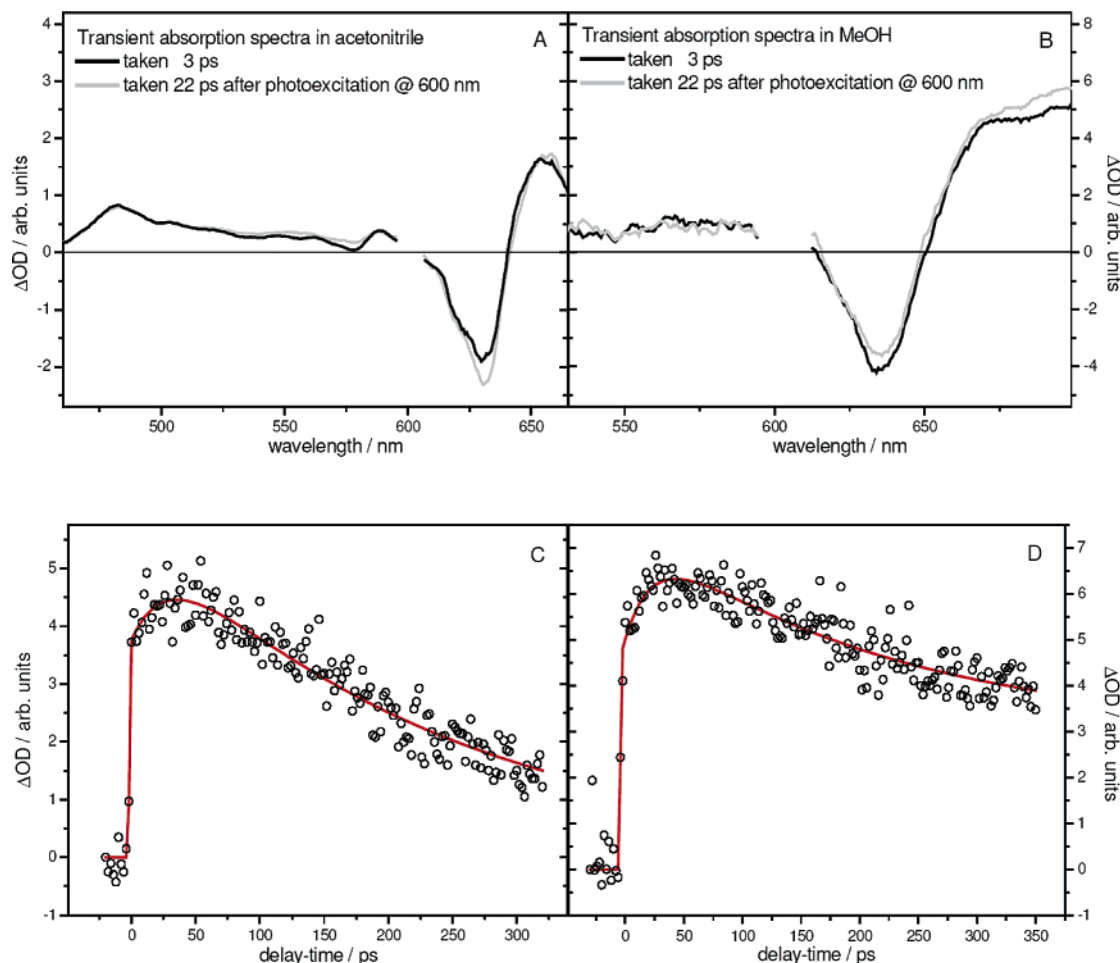


Figure 3. Difference absorption spectra and kinetics of the absorption changes of protochlorophyllide a in methanol and acetonitrile: (top) transient absorption spectra of protochlorophyllide a in acetonitrile (A) and methanol (B) taken 3 and 22 ps after excitation at 600 nm with 100 fs pulses; (bottom) kinetics of the absorption changes recorded in acetonitrile at 650 nm and in methanol at 680 nm. The dots indicate the experimentally measured data, and the solid lines indicate the calculated functions from the best-fit parameters. The estimated time constants are as follows: $\tau_1 = 4.5 \pm 1.2$ ps, $\tau_2 = 22 \pm 4$ ps, and $\tau_3 = 200 \pm 60$ ps in the solvent acetonitrile and $\tau_1 = 4.0 \pm 1.0$ ps, $\tau_2 = 27 \pm 6$ ps, and $\tau_3 = 200 \pm 60$ ps in the solvent methanol.

formed in the different solvents. Figure 3 compares the transient absorption spectra of Pchl *a* in methanol and acetonitrile (Figure 3A,B), which were obtained 3 and 22 ps after excitation with 100 fs pulses at 600 nm, that is, at the blue wing of the energetically lowest lying Q band. The difference absorption spectra display a strong bleaching of the ground-state absorption, which appears as a negative band with a maximum at ~ 630 nm. On either side of the bleaching band, broad and, to a large extent, structureless transient absorptions appear, which are obviously due to excited-state absorptions (ESAs). The ESAs cover nearly the entire spectral region accessible to our measurements and are considerably stronger on the red side versus the blue side of the bleaching band. However, despite the weaker intensities, the absorption changes in the blue region show the shape of the high energetic Q absorption sub-bands, which evidently reflect the superposition of the ESA and the ground-state bleaching in the corresponding spectral region. This effect is especially worth noting in the shoulder, as seen in the ESA at 615 nm for Pchl *a* in acetonitrile.

For a detailed kinetic analysis, the time evolution of the positive absorption changes in the red spectral region was measured between 0 and 350 ps in acetonitrile and in methanol (Figure 3C,D). As is obvious, the two kinetic traces exhibit nearly identical profiles. Initially, an ultrafast instrument response-limited rise is followed by a slower rise kinetics, which then falls into a slow decay. The rise components induce an increase in the absorption changes up to ~ 40 ps in either solvent. For further analysis, the kinetics was fitted to a multiexponential function convoluted with the instrumental response function. Following the best-fit results, the kinetics is composed of contributions from three exponential components including a constant term, which was introduced to simulate the nanosecond lifetime of the thermally equilibrated S_1 state, as it cannot be temporally resolved on the time scale of our measurements. In acetonitrile, the time constants τ_1 , τ_2 , and τ_3 were found to be equal to 4.5 ± 1.2 , 22 ± 4 , and 200 ± 60 ps, respectively, while the values in methanol are equal to 4.0 ± 1.0 , 27 ± 6 , and 200 ± 60 ps and thus correspond very well to those determined in our preceding letter.⁸ When compared, the time constants estimated for the solvents acetonitrile and methanol, which are very similar in their polarity and viscosity but different in their protic/aprotic properties, are in close agreement, suggesting that the protic/aprotic properties of the solvent environment are not an important factor in controlling the excited-state dynamics of Pchl *a*. In contrast to methanol and acetonitrile, the relaxation dynamics is substantially modified in cyclohexane solutions. Figure 4A shows the corresponding absorption difference spectrum of Pchl *a* in the nonpolar cyclohexane, monitored 1.5 and 5 ps after excitation into the lowest lying Q band at 620 nm. As can clearly be seen, the spectra are similar in their appearance to those obtained in the other two solvents with a strong ground-state bleaching in the region of the $S_0 \rightarrow S_1$ absorption accompanied by broad and less structured ESAs, which extend at the blue and red sides (not shown) of the bleaching band. The shift in the peak of the ground-state bleaching from 640 nm at the 1.5 ps time delay to 630 nm at the 5 ps time delay is typically the kind of spectral change brought about by a molecule cooling process due to the solvent-induced dissipation of excess vibrational energy within the S_1 excited state. That is, to the extent that the vibrational energy is redistributed and the S_1 state population decays along the vibrational ladder, the strong ESA in the red is blue-shifted, which finally also results in a blue shift of the maximum of the negative absorption band due to the spectral overlap between

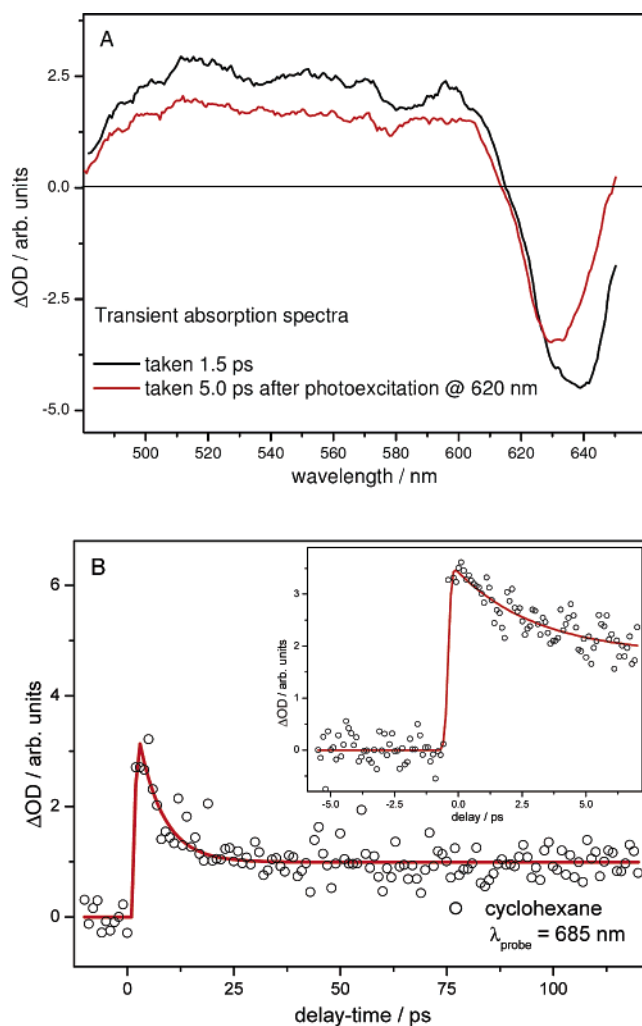


Figure 4. Difference absorption spectra and kinetics of the absorption changes of protochlorophyllide *a* in cyclohexane: (A) transient absorption spectra taken 1.5 and 5 ps after excitation at 620 nm with 100 fs pulses; (B) kinetics of the absorption changes recorded at 685 nm. The inset in part B shows the initial kinetics at an enlarged time scale. The dots indicate the experimentally measured data, and the solid line indicates the decay function calculated from the best-fit parameters. The decay is best fitted by a time constant of $\tau_1 = 4.5 \pm 1.8$ ps in addition to a long nanosecond decay time which is approximated as a constant term in the time window of the femtosecond measurements.

the ESA and ground-state bleaching. Figure 4B reveals the temporal evolution of the absorption changes at 685 nm, that is, in the region of the red ESA, as a representative example for the kinetics in the whole spectral range covered by ESAs. It shows the instrument response-limited rise and the subsequent decay. The kinetic data can be fit reasonably well with a single exponential component and a constant term. While the latter reflects the decay time of the long-lived thermally equilibrated S_1 state, the estimate of 4.5 ± 1.8 ps for the exponential component correlates well with the 4.0 and 4.5 ps estimates found for the fastest kinetics in methanol and acetonitrile solutions. However, the relaxation via the 22–27 and 200 ps decay channel is clearly not discernible. In this respect, the kinetics in the nonpolar environment diverges from that in the polar environment. Obviously, only in polar solvents, an additional route for deactivation from the S_1 excited state is available which yields an intermediate product that in turn undergoes relaxation back into the ground state in 200 ps. The strong influence of the solvent polarity on the population dynamics of the intermediate product suggests that it exhibits a

large dipole moment and therefore is stabilized by the polar solvent environment. On the basis of the chemical structure of Pchl *a*, that is, especially of the cyclopentanone ring connected as an electron withdrawing group directly to the π -electron conjugation path (Figure 1), it seems very likely that the highly dipolar character is due to an intramolecular charge transfer state (S_{ICT}), which becomes populated within the excited-state manifold in proximity to the S_1 excited state. The occurrence of an intramolecular charge transfer state on the excited-state hypersurface is a well-known phenomenon and is described as a common feature in the excited-state dynamics of carotenoids when these are substituted with electron withdrawing groups in conjugation with the carbon–carbon conjugated chain.^{13–16} Further, owing to the stabilization by the polar environment, it can be assumed that the S_{ICT} state lies in energy below the S_1 state so that the initially excited state can be depopulated via two decay channels either directly into the ground state or by passing the 22–27 ps state into the S_{ICT} state. As outlined in our previous letter,⁸ the 22–27 ps state most probably represents a secondary excited state (S_X) on the S_1 potential energy hypersurface. This can be concluded from the decay-associated spectrum of the 22–27 ps component, which is reported there. This spectrum, which is related to the depopulation of the S_X state, reveals strong negative contributions in the spectral region where stimulated emission is observed, thus indicating that the S_X state is fluorescent and most likely represents an excited electronic state. Another fact, which speaks in favor of this classification, is that a 27 ps decay component can be identified immediately after excitation in our very recent time-resolved fluorescence experiments (to be published). Compared with the polar solvent case, in the nonpolar solvent, the S_{ICT} state lies in energy above the S_1 state, thus increasing the energy barrier between the potential energy surfaces of the S_1 and S_{ICT} states. This barrier seems to be high enough to prevent the transfer into the S_{ICT} state. Apparently, for this reason, only the $S_1 \rightarrow S_0$ relaxation occurs, that is, the initial fast cooling process and the relaxation back into the ground state with the nanosecond time constant. A schematic representation of this reaction model is shown in Figure 7. It is addressed in more detail in a later paragraph together with additional experimental evidence presented below.

Pump Energy Dependency of the Excited-State Dynamics.

To obtain a closer picture of the relaxation dynamics in the S_1 state of Pchl *a*, this dynamics was also examined in the polar solvent environment as a function of the pump wavelength. In these experiments, the excitation wavelength was varied from 600 to 655 nm, that is, from the high energy edge to the low energy edge of the Q absorption band. Figure 5 compares two representative kinetics recorded in the region of the red ESA after excitation at 600 and 655 nm, respectively. The two kinetics do not exhibit any striking difference at delay times longer than 60 ps. However, excitation at 600 nm, which represents excitation into the higher vibrational levels, results in significantly faster early-time dynamics between 0 and 60 ps. The respective kinetic profile exhibits an instantaneous decay within a few picoseconds, which escapes detection under the 655 nm excitation, and a subsequent rise, which is also considerably faster compared to the 655 nm excitation. Kinetic analysis with the three-exponential model shows that the initial fast decay occurs with the time constant τ_1 of 4.0 ± 1.0 ps over the whole range of the excitation wavelengths, whereas the relative decay amplitude is drastically reduced as the excitation approaches the red edge of the Q absorption band. This kinetic behavior is again consistent with the suggested

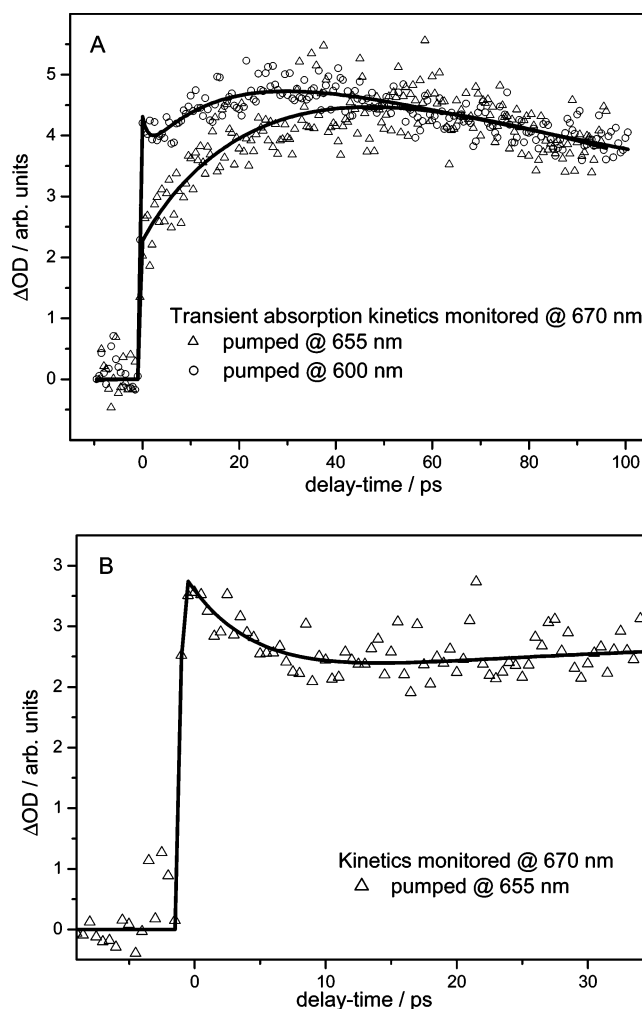


Figure 5. Transient absorption kinetics of protochlorophyllide *a* in methanol solution as a function of the excitation wavelength: (A) Kinetics measured in the time interval between 0 and 350 ps after excitation with 600 nm (○) and 655 nm (△) excitation pulses. The solid lines represent the best fits of the experimental data to the three-exponential fit function. The kinetics are best fitted by time constants of $\tau_1 = 4.0 \pm 1.0$ ps and $\tau_3 = 200 \pm 60$ ps for excitation at the two excitation wavelengths as well as $\tau_2 = 19 \pm 2$ ps for excitation at 600 nm and $\tau_2 = 27 \pm 3$ ps for excitation at 655 nm. (B) Enlargement of the early-time dynamics.

assignment of the 4 ps component to vibrational cooling of the S_1 state. It is expected that the fractional contribution of vibrational cooling to the overall decay processes drops off with a decrease in the excess vibrational energy delivered to the molecular system by the pump photons. In contrast to molecular cooling associated with τ_1 , the rise kinetics of the intermediate state, related to τ_2 , becomes appreciably slower with excitation into the red tail of the Q absorption band and varies between 19 ± 2 ps for excitation at 600 nm and 27 ± 3 ps for excitation at 655 nm. Finally, the slower decay kinetics is characterized by the 200 ± 60 ps time constant, which corresponds to τ_3 , and which, similar to τ_1 , remains approximately equal over the whole range of excitation wavelengths. The observed dependency of τ_2 on the excitation wavelength suggests that the 19–27 ps state and the S_{ICT} state are separated from each other by an energy barrier obviously due to the displacement of the potential energy minimum of the S_{ICT} state along the reaction coordinate. This energy barrier prevents the quasi-instantaneous population of the S_{ICT} state but can be overcome more easily, the higher the excess vibrational energy of the excitation photon is. Thus, excitation into the higher vibrational levels of the S_1

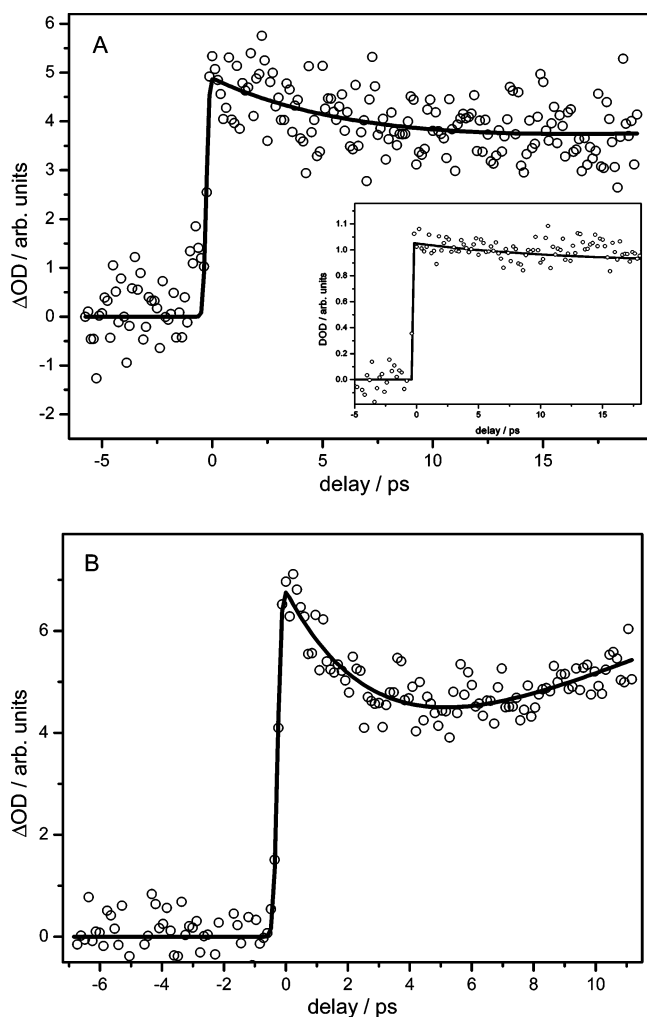


Figure 6. Transient absorption changes of protochlorophyllide a in solvents of different viscosities: (A) Kinetic absorption changes measured at 495 nm (region of the blue excited-state absorption) in a mixture of methanol/glycerol (40/60). To visualize the prolongation of the kinetics also in the region of the red ESA, the inset shows the kinetic absorption changes monitored at 670 nm. (B) Kinetic absorption changes measured at 680 nm (region of the red excited-state absorption) in the solvent methanol. The dots indicate the experimentally measured data, and the solid line indicates the decay function calculated from the best-fit parameters. The kinetics are best fitted by time constants of $\tau_1 = 12.1 \pm 2.6$ ps, $\tau_2 = 40 \pm 7$ ps, and $\tau_3 = 270 \pm 70$ ps for the mixture of methanol/glycerol (40/60) as well as $\tau_1 = 4.0 \pm 1.0$ ps, $\tau_2 = 27 \pm 6$ ps, and $\tau_3 = 200 \pm 60$ ps for the solvent methanol.

state increases the transition rate, while it is remarkably reduced when the S_{ICT} state is populated from the lower vibrational states. The enhanced transition rate may further be explained by a stronger vibronic coupling between the 19–27 ps state and the S_{ICT} state, when excitation leads to the population of higher excited vibrational modes. Then, in general, it holds that the absolute estimate of the nonadiabatic coupling matrix element in the form of $\langle f(v_f) | \partial^2 / \partial x^2 | i(v_i) \rangle$ increases with an increasing quantum number of the vibrational states involved in the respective transition. Moreover, the rate of the nonadiabatic crossing also depends on the density of the vibrational states in the final energy potential. As the density of states increases with increasing energy, this effect gives further rise to an acceleration of the $S_1 \rightarrow S_{ICT}$ transition rate and, in turn, to a shortening of the associated time constant τ_2 .

Effects of Solvent Viscosity on the Excited-State Dynamics.

In order to explore the role of specific excited-state nuclear displacements in the formation of the intramolecular charge

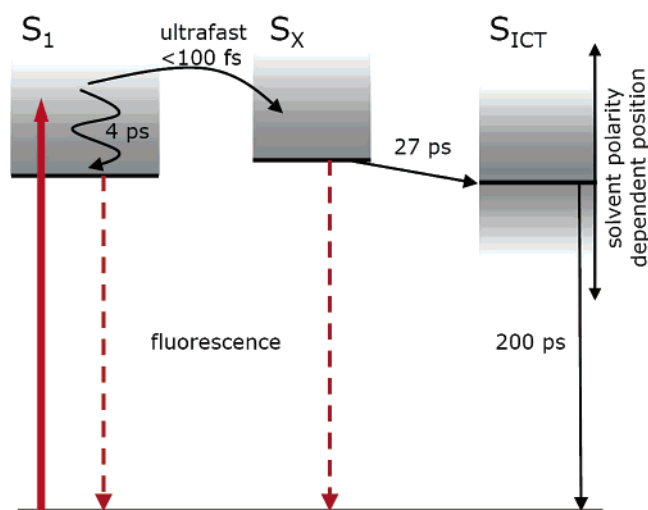


Figure 7. Level scheme suggested for the excited-state dynamics in protochlorophyllide a. S_X denotes a secondary S_1 excited state on the S_1 potential energy surface and S_{ICT} an intramolecular charge transfer state. For more details, see text.

transfer state, the effect of the solvent viscosity on the excited-state dynamics was studied. For this purpose, the solvent methanol was substituted by a methanol/glycerol (40/60) mixture that does not significantly differ in its polarity factor from the pure methanolic solution but exhibits a remarkably increased solvent viscosity (Table 1). In Figure 6, the kinetics of the absorption changes at 495 nm in the methanol/glycerol mixture versus the absorption changes at 680 nm in pure methanol is shown for the first 12–15 ps after excitation. The two kinetics represent the time evolution of ESAs. In the methanol/glycerol mixture, as in pure methanol, ESA bands appear both on the blue and red sides of ground-state bleaching. Both exhibit the same dynamics, thereby enabling the comparison of the kinetics for the blue ESA in the methanol/glycerol mixture with the red ESA in pure methanol. As evident from Figure 6, the kinetics in the two solvents varies significantly. In the higher viscosity methanol/glycerol mixture, it is dominated by a 12 ps decay in the first 12–15 ps after excitation, whereas, in pure methanol, the initial dynamics exhibits the fast 4 ps decay, which is followed by a slower rise component with the 27 ps time constant. Fitting the kinetic data acquired in the methanol/glycerol mixture over a longer time interval and wider spectral region leads to three exponential components with time constants of $\tau_1 = 12.1$ ps, $\tau_2 = 40$ ps, and $\tau_3 = 270$ ps that contribute to the overall kinetics. In Table 1, the respective time constants and, for comparison, the corresponding estimates for the other solvents used in this study are summarized together with the polarity and viscosity factors of the solvents. With regard to the 12 and 40 ps components, a remarkable lengthening from the values in methanol occurs, while the slower 270 ps component remains virtually unaffected by the solvent viscosity when the experimental error is taken into account. The prolongation of the 4 ps time constant in methanol to 12 ps in the methanol/glycerol solution reveals that the process of vibrational cooling is controlled by the solvent viscosity. In addition, the 27 ps process is also slowed to 40 ps when the solvent viscosity is increased, thus indicating that this process is accompanied by nuclear motions along a reaction coordinate. At present, we do not know the reason for the viscosity sensitivity of this process. However, it is known that some nonplanar porphyrins have a propensity for photoinduced conformational changes.^{17–19} It is therefore tempting to speculate that the 27 ps kinetics reflects an excited-state conformational

transition in the porphyrin macrocycle that is associated with the formation of the S_{ICT} state. Further investigations are required in order to establish the molecular nature of this relaxational process definitely.

Model of the Excited-State Dynamics and Conclusions

The results presented above clearly show that the excited-state dynamics of Pchl *a* strongly depends on solvent polarity. While in the polar solvents methanol and acetonitrile the transient absorption kinetics is composed of three kinetic components with time constants of 4.0–4.5 ps (τ_1), 22–27 ps (τ_2), and 200 ps (τ_3), only the fast 4.5 ps component can be observed in the nonpolar solvent cyclohexane. For the following reasons, this ~ 4 ps component is very likely related to vibrational energy redistribution and vibrational cooling of the initially excited S_1 state: (i) the decay of this component gives rise to a characteristic blue shift in the ESA, extending from the red tail of ground-state bleaching, accompanied by a blue shift in ground-state bleaching itself; (ii) the decay amplitude is significantly reduced for excitation at the red versus the blue tail of the Q absorption band; and (iii) it appears in the excited-state dynamics independent of the specific solvent conditions. While under the nonpolar solvent conditions the ~ 4 ps process leads to thermal equilibrium in the S_1 excited state followed by the repopulation of the initial ground state on the nanosecond time scale, a parallel reaction path, which generates a new intermediate state, seems to be opened under the polar solvent conditions. A simple scheme for the illustration of this de-excitation pathway is shown in Figure 7. On the basis of the observed excited-state dynamics, the new intermediate state, S_{ICT} , is built up by the 22–27 ps process. Considering the low fluorescence yield ($\Phi_{\text{fluorescence}} = 0.06 \pm 0.01$),⁸ the corresponding electronic state, S_X , most probably results from a very fast motion out of the Franck–Condon region into the reactive path. The appearance of a long-wavelength stimulated emission in the decay-associated spectrum of the S_X state, as shown in our previous letter,⁸ suggests that this state belongs to an excited electronic state, which most likely exists as a local minimum on the S_1 potential energy surface. The results of recent time-resolved fluorescence measurements (to be published) further support this suggestion in that they indicate the presence of a fluorescence component with a lifetime similar to the 22–27 ps kinetics in the absorption measurements reported here. The S_X state is then able to react to the intermediate state, S_{ICT} , which decays back to the original ground state with a time constant of 200 ps. The S_X state and the S_{ICT} state appear to be separated by an energy barrier. This can be concluded from a distinct prolongation of the time constant for the $S_X \rightarrow S_{ICT}$ transition when the excitation energy is decreased (19 ± 2 ps for excitation at 600 nm vs 27 ± 3 ps for excitation at 655 nm).

The opening of the reactive path only in polar solvents indicates that the polar environment is a prerequisite for the formation of the intermediate S_{ICT} state. It is therefore suggested that the S_{ICT} state has a large dipole moment and most likely represents an intramolecular charge transfer state. On the basis of the molecular structure of Pchl *a*, the charge transfer state could result from the electron withdrawing effect of the carbonyl group within the cyclopentanone ring attached directly to the π -electron conjugation path of the porphyrin ring system. Most probably, in nonpolar solvents, the energy of the charge transfer state is significantly raised, thus preventing the transfer of the excited-state population toward the S_{ICT} state. Additional support for the assignment of the intermediate S_{ICT} state to an intramolecular charge transfer state is obtained by our recent time-

resolved studies on magnesium octaethylporphyrin (MgOEP).²³ In contrast to Pchl *a*, no intermediate S_{ICT} state is generated in the excited-state decay of MgOEP under polar solvent conditions. Following excitation, only the direct repopulation of the original ground state can be observed. The chemical structure of MgOEP is similar to that of Pchl *a* at least with respect to the magnesium porphyrin macrocycle, which makes up the chromophoric system in the two compounds. Differences occur in the peripheral substituents. In particular, the cyclopentanone ring connected directly to the conjugated π -electron path in Pchl *a* is missing in MgOEP. It appears that the absence of the cyclopentanone ring, acting as an electron acceptor in the charge transfer complex, prevents the population of the intermediate S_{ICT} state in the excited-state decay of MgOEP.

From the excited-state dynamics of Pchl *a*, it is further evident that the reaction rate of the processes attributed to vibrational cooling as well as to the $S_X \rightarrow S_{ICT}$ relaxation is significantly reduced when the solvent viscosity is increased. The time constant for the $S_X \rightarrow S_{ICT}$ relaxation is slowed from 27 ± 6 ps in methanol to 40 ± 7 ps in a methanol/glycerol (40/60) mixture. While the slowing of the time constant for vibrational cooling can be expected in a higher viscous medium, the viscosity effect on the $S_X \rightarrow S_{ICT}$ relaxation rate might reflect a conformational change in the structure of the porphyrin macrocycle, which accompanies the formation of the intramolecular charge transfer state. Finally, the S_{ICT} state is depopulated to the ground state with a 200 ps time constant. This relaxation process remains unaffected by solvent viscosity within the limits of experimental error.

Given the above results, it seems likely that the enzyme-catalyzed photoreduction of Pchl *a* in the NADPH/protochlorophyllide oxidoreductase is also strongly influenced by the protein environment in the substrate binding pocket. Further, from the remarkable similarity in the time constants of 400 ps for the photoreduction of Pchl *a* in the enzyme complex⁷ and of 200 ps for the decay of the intermediate product in the reaction path of free Pchl *a*, it is tempting to speculate (i) that the enzyme-catalyzed reaction is controlled by the polarity of the protein environment and (ii) that an intramolecular charge transfer complex plays a significant role in the excited-state reaction dynamics of the enzyme-bound Pchl *a*.

Acknowledgment. This work was financially supported by the Deutsche Forschungsgemeinschaft, through the grant Sonderforschungsbereich 436 (Metallvermittelte Reaktionen nach dem Vorbild der Natur, TP C1). B.D. highly acknowledges financial support from the Studienfonds der Chemischen Industrie.

References and Notes

- (1) Suzuki, J. Y.; Bolivar, D. W.; Bauer, C. E. *Annu. Rev. Genet.* **1997**, *31*, 3161.
- (2) Beale, S. *Photosynth. Res.* **1999**, *60*, 43.
- (3) Rüdiger, W. In *The Porphyrin Handbook*; Kadish, K. M., Smith, K. M., Guillard, R., Eds.; Academic Press: Amsterdam, Boston, London, New York, 2003; Vol. 13, p 71.
- (4) Schoefs, B.; Franck, F. *Photochem. Photobiol.* **2003**, *78*, 543.
- (5) Masuda, T.; Takamiya, K. *Photosynth. Res.* **2004**, *81*, 1.
- (6) Yang, J.; Cheng, Q. *Plant Biol.* **2004**, *6*, 537.
- (7) Heyes, D. J.; Hunter, C. N.; van Stokkum, I. H. M.; van Grondelle, R. *Nat. Struct. Biol.* **2003**, *10*, 491.
- (8) Dietzek, B.; Maksimenka, R.; Siebert, T.; Birckner, E.; Kiefer, W.; Popp, J.; Hermann, G.; Schmitt, M. *Chem. Phys. Lett.* **2004**, *397*, 110.
- (9) Siebert, T.; Maksimenka, R.; Materny, A.; Engel, V.; Kiefer, W.; Schmitt, M. *Raman Spectrosc.* **2002**, *33*, 844.

- (10) Klement, H.; Helfrich, M.; Oster, U.; Schoch, S.; Rüdiger, W. *Eur. J. Biochem.* **1999**, 265, 862.
- (11) Gouterman, M. In *The Porphyrins*; Dolphin, D., Ed.; Academic Press: New York, 1978; Vol. 3, p 1.
- (12) Mysliwa-Kurdziel, B.; Kruk, J.; Strzalka, K. *Photochem. Photobiol.* **2004**, 79, 62.
- (13) Bautista, J. A.; Connors, R. E.; Raju, B. B.; Hiller, R. G.; Sharples, F. P.; Gosztola, D.; Wasielewski, M. R.; Frank, H. A. *J. Phys. Chem. B* **1999**, 103, 8751.
- (14) Frank, H. A.; Bautista, J. A.; Josue, J.; Pendon, Z.; Hiller, R. G.; Sharples, F. P.; Gosztola, D.; Wasielewski, M. R. *J. Phys. Chem. B* **2000**, 104, 4569.
- (15) Zigmantas, D.; Polivka, T.; Hiller, R. G.; Yartsev, A.; Sundström, V. *J. Phys. Chem. A* **2001**, 105, 10296.
- (16) Zigmantas, D.; Hiller, R. G.; Yartsev, A.; Sundström, V.; Polivka, T. *J. Phys. Chem. B* **2003**, 107, 5339.
- (17) Gentemann, S.; Nelson, N. Y.; Jaquinod, L.; Nurco, D. J.; Leung, S. H.; Medforth, C. J.; Smith, K. M.; Fajer, J.; Holten, D. *J. Phys. Chem. B* **1997**, 101, 1247.
- (18) Retseck, J. L.; Gentemann, S.; Medforth, C. J.; Smith, K. M.; Chirvony, V. S.; Fajer, J.; Holten, D. *J. Phys. Chem. B* **2000**, 104, 6690.
- (19) Enescu, M.; Steenkeste, K.; Tfibel, F.; Fontaine-Aupart, M.-P. *Phys. Chem. Chem. Phys.* **2002**, 4, 6092.
- (20) Laermer, F.; Elsaesser, T.; Kaiser, W. *Chem. Phys. Lett.* **1989**, 156, 381.
- (21) Yu, H.-Z.; Baskin, J. Sp.; Zewail, A. H. *J. Phys. Chem. A* **2002**, 106, 9845.
- (22) Baskin, J. Sp.; Yu, H.-Z.; Zewail, A. H. *J. Phys. Chem. A* **2002**, 106, 9837.
- (23) Dietzek, B.; Maksimenka, R.; Kiefer, W.; Hermann, G.; Popp, J.; Schmitt, M. *Chem. Phys. Lett.* **2005**, 415, 94.